frontiers in Energy Research

ORIGINAL RESEARCH
published: 13 December 2017
doi: 10.3389/fenrg.2017.00033

Nickel Nanowire@Porous $NiCo_2O_4$ Nanorods Arrays Grown on Nickel Foam as Efficient Pseudocapacitor Electrode

*Houzhao Wan, Lang Li, Jun Zhang, Xiang Liu, Hanbin Wang and Hao Wang**

Faculty of Physics and Electronic Science, Hubei Collaborative Innovation Center for Advanced Organic Chemical Materials, Hubei Key Laboratory of Ferro & Piezoelectric Materials and Devices, Hubei University, Wuhan, China

A three dimensional hierarchical nanostructure composed of nickel nanowires and porous $NiCo_2O_4$ nanorods arrays on the surface of nickel foam is successfully fabricated by a facile route. In this structure, the nickel nanowires are used as core materials to support high-pseudocapacitance $NiCo_2O_4$ nanorods and construct the well-defined $NiCo_2O_4$ nanorods shell/nickel nanowires core hierarchical structure on nickel foam. Benefiting from the participation of nickel nanowires, the nickel nanowire@$NiCo_2O_4$/Ni foam electrode shows a high areal specific capacitance (7.4 F cm^{-2} at 5 mA cm^{-2}), excellent rate capability (88.04% retained at 100 mA cm^{-2}), and good cycling stability (74.08% retained after 1,500 cycles). The superior electrochemical properties made it promising as electrode for supercapacitors.

Keywords: nickel nanowire, core-shell, nickel–cobalt oxide, nanorod, supercapacitor

OPEN ACCESS

Edited by:
Mariusz Walkowiak, Institute of Non-Ferrous Metals, Poland

Reviewed by:
Huan Pang, Yangzhou University, China
Chunming Zhang, National Engineering Research Center for Nanotechnology, China

***Correspondence:**
Hao Wang
nanoguy@126.com

Specialty section:
This article was submitted to Energy Storage, a section of the journal Frontiers in Energy Research

Received: *17 August 2017*
Accepted: *27 November 2017*
Published: *13 December 2017*

Citation:
Wan H, Li L, Zhang J, Liu X, Wang H and Wang H (2017) Nickel Nanowire@Porous $NiCo_2O_4$ Nanorods Arrays Grown on Nickel Foam as Efficient Pseudocapacitor Electrode. Front. Energy Res. 5:33. doi: 10.3389/fenrg.2017.00033

INTRODUCTION

Developing high-performance electrochemical energy storage devices has been one of the important issues in the energy strategic projects established all over the world (Li et al., 2017a,b,c; Wei et al., 2017; Xia et al., 2017). Among various energy storage devices, electrochemical capacitors (called as supercapacitors), with high power density, fast charge–discharge rate, and long lifespan, are considered typically as one of the most appropriate choice energy storage and conversion devices (Li et al., 2017a,b,c; Sun et al., 2017; Zheng et al., 2017a,b). According to the mechanism of charge storage, it is significantly that they not only have a large surface area for improving double-layer capacitance, but also offer a short diffusion length for abundant redox reactions, which is important for pseudocapacitance (Deng et al., 2017; Kim et al., 2017; Zheng et al., 2017a,b). Among metal compounds, binary nickel–cobalt oxides attract the extensive attention for their relatively high electrochemical performance (Li et al., 2015). For instance, the three dimensional (3D) hierarchical flower-shaped $NiCo_2O_4$ microsphere exhibited 1006 F g^{-1} at 1 A g^{-1}, enhanced rate capability and excellent electrochemical stability (Lei et al., 2014). Lou et al. reported that the $NiCo_2O_4$ hollow spheres show 1141 F g^{-1} at 1 A g^{-1} and enhanced cycling stability (Shen et al., 2015). Furthermore, to maximize pseudocapacitor, one needs to construct a porous structure with a large number of active sites, and other one can design a conducting channel with high transport rates of electrons and electrolyte ions (Yuan et al., 2012).

To further improve the charge transport aiming at the intrinsic poor electrical conductivity of metal compounds, the development of electrodes with ordered nanoarrays grown directly on a collector [such as Ni foam (Li et al., 2018), Cu foil (Zhang et al., 2012; Cheng et al., 2015), Ti

foil (Lu et al., 2011), and carbon cloth (Li et al., 2017a,b,c)] without any binders is particularly significant for charge storage of electrochemically inactive (Chen et al., 2017; Liu et al., 2017; Shi et al., 2017). For example, MnO_2 nanowire/CNT paper electrode display 167.5 F g^{-1} at 77 mA g^{-1} (Chou et al., 2008). $Ni(OH)_2$ nanoflakes/Ni foam delivers 1228 F g^{-1} and 918 F g^{-1} at 5 A g^{-1} and 30 A g^{-1}, respectively, with excellent cycling stability (Hu et al., 2013). $NiCo_2S_4$ nanotube/nickel foam shows 738 F g^{-1} at 4 A g^{-1} (Pu et al., 2014). Nickel–cobalt hydroxide nanoarrays/carbon nanofibers reveal 1378.2 F g^{-1} for nanorod arrays and 1195.4 F g^{-1} for nanosheet arrays at 1 A g^{-1} (Lai et al., 2015). $NiCo_2O_4$ nanoneedles on Ni foam and Ti foil binder-free electrode exhibit greatly improved electrochemical performance (Zhang et al., 2012). This electrode design renders other auxiliary components such as conductive agent and binder completely unnecessary to allow for more efficient charge and mass exchange.

Three dimensional hierarchical hybrid nanostructures composed of high conductive core materials and high-performance shell materials are promising electrode architectures for superior supercapacitors (Xiao et al., 2012; Tang et al., 2013). Herein, we first successfully fabricated a novel 3D hierarchical hybrid electrode composed of nickel nanowires@porous $NiCo_2O_4$ nanorods arrays core–shell structure aligned on nickel foam (NiNW@$NiCo_2O_4$/NF) by a facile route. In this structure, the nickel nanowires are used as high conductive core materials to support high-pseudocapacitance porous $NiCo_2O_4$ nanorods shell materials, and the integrated nickel nanowire/Ni foam (Ni NW/NF) composite substrate work as an excellent binder-free current collector. Benefited from the design of 3D hierarchical core–shell nanostructure, the resulting NiNW@$NiCo_2O_4$/NF electrode exhibits excellent electrochemical properties for supercapacitors.

EXPERIMENTAL SECTION

Preparation of Integrated Ni Nanowire/Ni Foam Composite Substrate

The integrated NiNW/NF composite substrate was synthesized by a simple water bath method. A prepared solution of $NiCl_2$ aqueous solution (0.05 M, 50 mL) was mixed with tritonX-100 aqueous solution (0.05 M, 50 mL), and a piece of pre-prepared nickel foam was added and treated with ultrasonication for several minutes. After that, the container containing the mixed solution was transferred to the water bath pot and heated up to 75°C. Next the mixed solution of 5 mL $N_2H_4.H_2O$ (85%) with 0.3 mL NaOH solution (1 M) was added. After 1.5 h, the Ni foam coated with a layer of black and fluffy NiNW was obtained, then washed and dried for next step.

Synthesis of Ni Nanowire@$NiCo_2O_4$/Ni Foam

The $NiCo_2O_4$ nanorods were grown on the NiNW/NF composite substrate by a typical hydrothermal method. First, the as-prepared NiNW/NF composite substrate was placed vertically in 100 mL Teflon lining. After that, the well-prepared mixed solution of 0.75 mmol $NiCl_2.6H_2O$, 1.5 mmol $CoCl_2.6H_2O$, and 4.5 mmol urea in the 60 mL deionized water was added, and then heated at 120°C for 8 h. After being cooled to room temperature, the product of NiNW@NiCo-precursor/NF was collected, cleaned and dried for further use. Finally, the NiNW/NF with the as-grown precursor was annealed at 350°C for 2 h in air with a heating rate of 1°C/min to obtain Ni nanowire@$NiCo_2O_4$/Ni foam electrode.

Materials Characterization

The phase was characterized by X-ray diffraction (XRD, advanced D8) with Cu Kα radiation. The morphology of the samples were observed by scanning electron microscope (SEM, JEOL JSM-7100F, FSEM/EDS). The structures of core/shell were investigated by means of transmission electron microscopy (TEM, FEI Tecnai 20). The surface structure and bonding environment of samples were examined by XPS using Thermo Fisher Scientific Escalab 250Xi spectrometer with a monochromatic Al Kα source. Brunauer–Emmett–Teller (BET) surface areas and pore volumes were measured on a Micromeritics ASAP 2020 sorptometer using nitrogen adsorption at 77 K.

Electrochemical Measurements

A three-electrode system was applied to measure the response of 3D NiNW@$NiCo_2O_4$/NF as working electrode. The 6 M KOH, platinum plate, and Hg/HgO were employed as electrolyte, counter, and reference electrode, respectively. The performances for three-electrode configurations were measured with CHI 660E electrochemical station. The cyclic voltammetry (CV), galvanostatic charge–discharge technique, and electrochemical impedance spectroscopy were used to probe electrochemical performance of the electrodes.

RESULTS AND DISCUSSION

Figure 1 and Figure S1 in Supplementary Material show the XRD patterns of NF, Ni NW/NF, $NiCo_2O_4$/NF, and Ni NW@$NiCo_2O_4$/NF. Thereinto the strong diffraction, two peaks at $2\theta = 44.5$ and

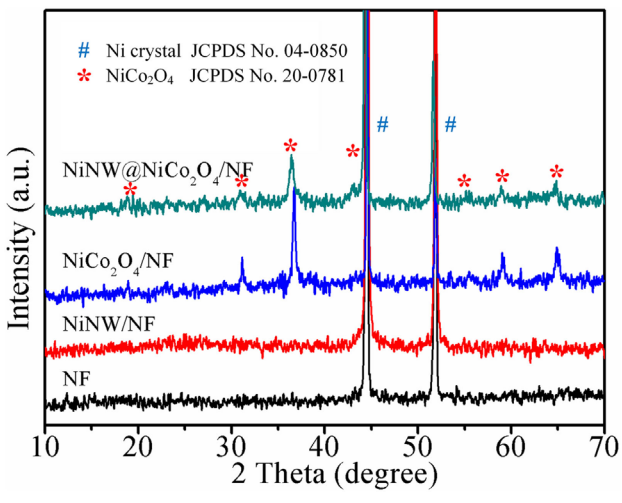

FIGURE 1 | The X-ray diffraction (XRD) patterns of NF, Ni NW/NF, $NiCo_2O_4$/NF, and Ni NW@$NiCo_2O_4$/NF.

51.8 correspond to the diffraction peaks of the Ni crystal from (111) and (200) (JCPDS No. 04-0850). The well-defined diffraction peaks observed at 2θ values of 19.2°, 31.3°, 36.9°, 44.7°, 54.1°, 59.3°, and 64.9° can be successfully indexed to (111), (220), (311), (400), (422), (511), and (440) planes of the cubic $NiCo_2O_4$ (JCPDS No. 73-1702). No other crystallized phases are detected, indicating the high purity.

The morphology of the samples was investigated by SEM, as shown in **Figure 2**. **Figure 2A** shows that the nickel nanowires are uniformly adhered on the surface of the nickel foam. All direction extending network structure composed of the uniform prickly nickel nanowires with the diameter of about 800 nm (**Figure 2D**). The growth of prickly nickel nanowires with lots of bumps on the surface of nickel foam can significantly increase the surface area which is beneficial to the deposition of active materials. The morphology of NiNW@NiCo-precursor/NF is presented in **Figures 2B,E**, the Ni nanowire is completely covered by the NiCo-precursor nanorods, which have diameters of 100 nm and lengths about 4 μm. The NiCo-precursor nanorods grow directly from the Ni nanowire surface forming an array structure. The morphology of NiNW@$NiCo_2O_4$/NF after annealing is presented in **Figures 2C,F**, it indicates the NiNW@$NiCo_2O_4$/NF with high-density $NiCo_2O_4$ nanorods are uniformly distributed on the Ni nanowire. Typical nanorods have the lengths of about 4 μm with diameters around 100 nm. Figure S2 in Supplementary Material shows the SEM images of $NiCo_2O_4$/NF. The TEM image shows that lots of pores appear after annealing and form the porous $NiCo_2O_4$ nanorods, as shown in **Figure 2G**. The porous nanostructure can further enrich the active site and, hence, to improve electrochemical properties. The formation schematic illustration of Ni NW@$NiCo_2O_4$/NF was presented in **Figure 2G**. The preparation process mainly involves three steps. In the first step, nickel nanowires are generated on nickel foam surface by chemical bath deposition. In the second step, Ni–Co precursor nanorods are grown on Ni nanowires by hydrothermal process. In the third step, Ni–Co precursor nanorods are thermally transformed to $NiCo_2O_4$ nanorods supported on the Ni nanowires.

X-ray photoelectron spectroscopy was further employed to characterize the valence state, as shown in **Figure 3**. The survey spectrum in **Figure 3A** indicates the presence of Ni, Co, and O.

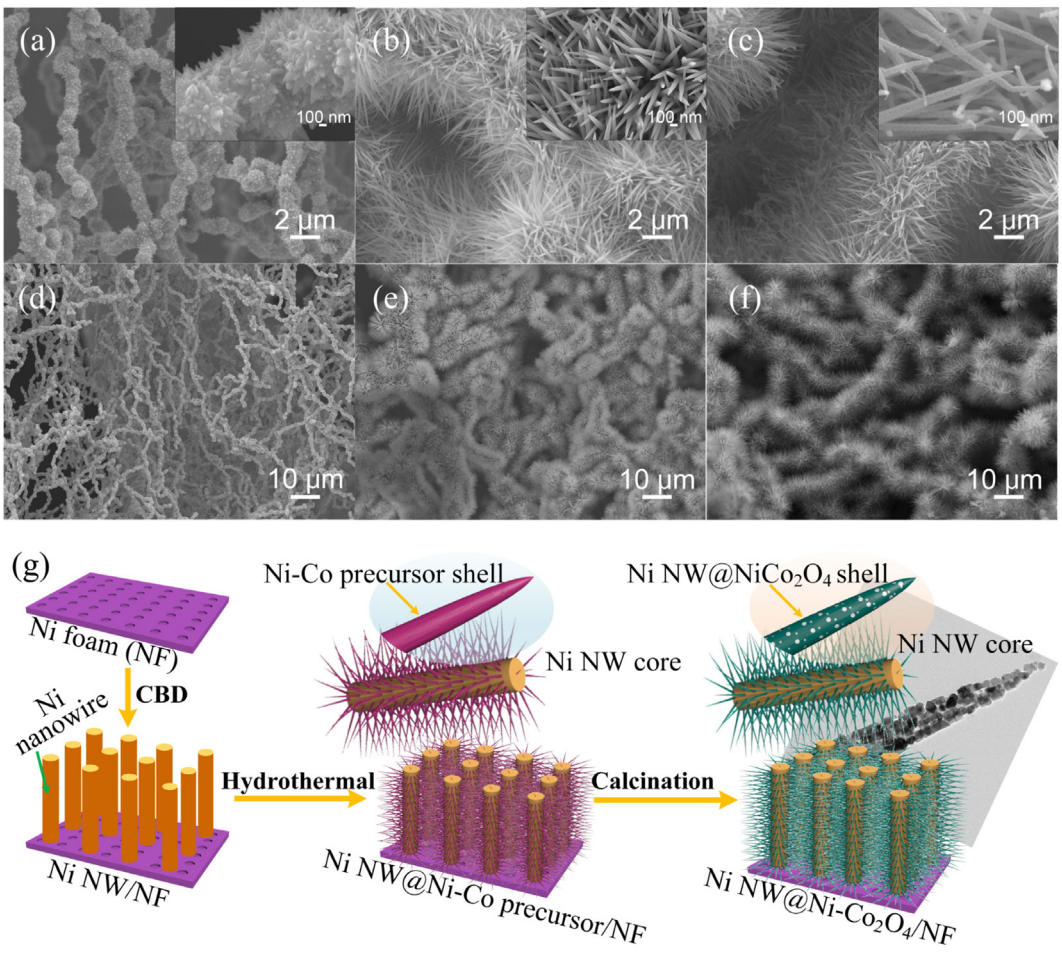

FIGURE 2 | **(A,D)** Scanning electron microscope (SEM) images of Ni MW/NF. **(B,E)** SEM images of Ni NW@Ni–Co precursor/NF. **(C,F)** SEM images of Ni NW@$NiCo_2O_4$/NF. **(G)** Formation mechanism of the Ni NW@$NiCo_2O_4$/NF.

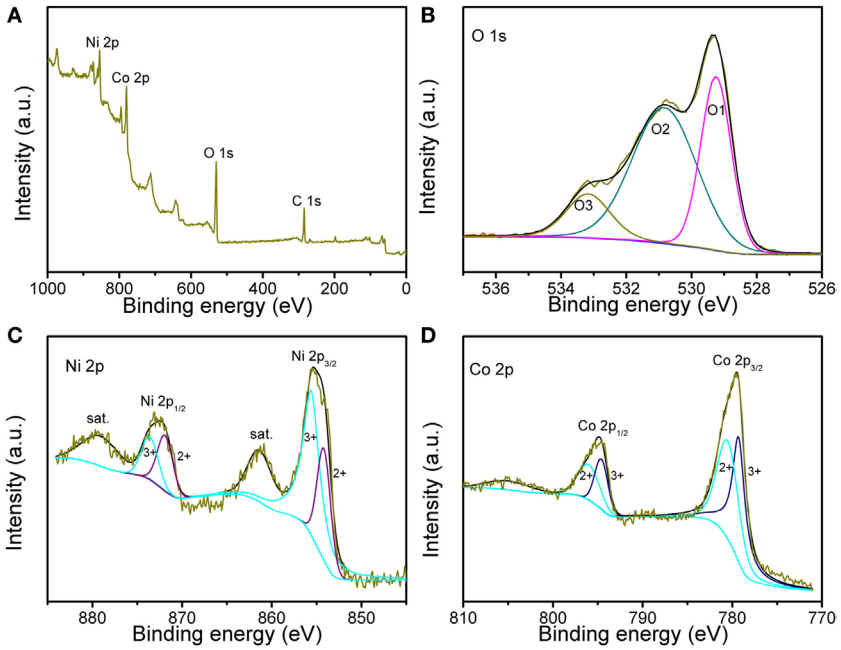

FIGURE 3 | X-ray photoelectron spectroscopy (XPS) spectra of **(A)** survey spectrum, **(B)** O 1 s, **(C)** Ni 2p, and **(D)** Co 2p regions for the sample.

The fitted fine spectra for the O 1 s, Ni 2p and Co 2p are obtained in **Figures 3B–D**, respectively. The O 1 s core level spectrum contains three peaks: O1, O2, and O3. The peaks of O1 at 529.3 eV and O2 at 530.8 eV are ascribed to the metal–oxygen and some defect sites with low oxygen coordination. The peak of O3 at 533.2 eV can be due to the physic-chemisorbed water. **Figure 3C** confirms the presence of Ni^{2+} and Ni^{3+}, thereinto the peaks at 854.2 and 871.9 eV are indexed to Ni^{2+}, while other peaks at 85.6 and 873.6 eV are from Ni^{3+}. As presented in **Figure 3D**, two types of Co species can be detected from Co 2p XPS spectrum. The peaks at 780.5 and 796.0 eV are belonged to Co^{2+}, while those at 779.3 and 794.0 eV are assigned to Co^{3+}. These results are well consistent with the reported $NiCo_2O_4$.

In order to probe into the above discussion of the Ni nanowire-based electrodes on the electrochemical properties, the specific surface areas of the $NiCo_2O_4$/NF and NiNW@$NiCo_2O_4$/NF were measured by BET. **Figure 4** shows the nitrogen adsorption and desorption isotherms of $NiCo_2O_4$/NF and NiNW@$NiCo_2O_4$/NF. The BET surface areas (SBET) of $NiCo_2O_4$/NF and NiNW@$NiCo_2O_4$/NF reveal 6.3 and 13.9 $m^2\ g^{-1}$. In addition, the average pore diameter obtained from Barrett–Joyner–Halenda (BJH) desorption isotherm is about 18.5 and 11 nm. Thereinto, the distribution of mesoporous of $NiCo_2O_4$/NF and NiNW@$NiCo_2O_4$/NF is similar from porous $NiCo_2O_4$ nanorods. The results show that the high specific surface area of the NiNW@$NiCo_2O_4$/NF is due to the addition of nickel nanowires.

Figure 5A shows the CV curves of the $NiCo_2O_4$/NF and NiNW@$NiCo_2O_4$/NF recorded at a scan rate of 5 mV s^{-1}. Distinct redox peaks which can be observed reveal the typical faradaic capacitance features of the electrodes. The relevant redox reactions related to M–O/M–O–OH (M refers to Ni or Co) which

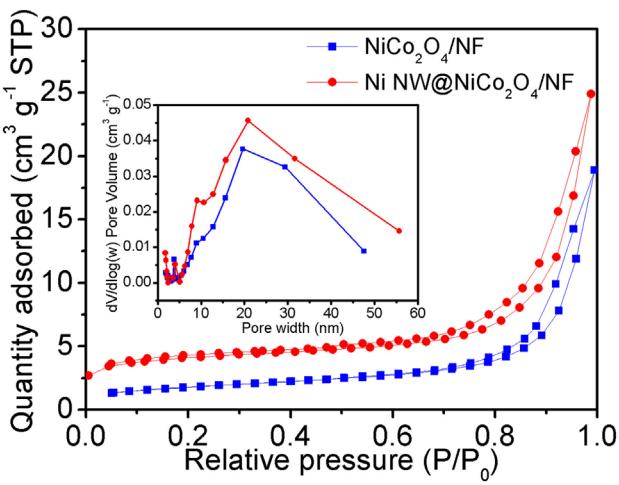

FIGURE 4 | Nitrogen adsorption and desorption isotherms measured at 77 K for the $NiCo_2O_4$/NF and NiNW@$NiCo_2O_4$/NF. The inset shows the corresponding Barrett–Joyner–Halenda (BJH) pore size distributions.

took place on the surface of electrodes in the alkaline electrolyte could be expressed as follows (Liu et al., 2013; Shang et al., 2017).

$$NiCo_2O_4 + OH^- + H_2O \rightleftharpoons NiOOH + 2CoOOH + e^- \quad (1)$$

$$CoOOH + OH^- \rightleftharpoons CoO_2 + H_2O + e^- \quad (2)$$

It can be observed that the NiNW@$NiCo_2O_4$/NF have the larger CV curve area than $NiCo_2O_4$/NF demonstrating the higher specific capacitance. And the galvanostatic charge–discharge

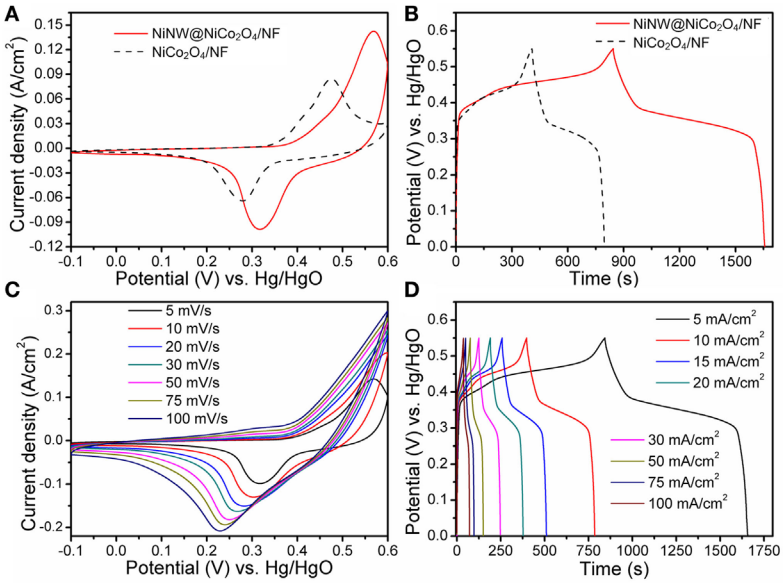

FIGURE 5 | **(A)** Cyclic voltammetry (CV) curves at 5 mV s^{-1} and **(B)** galvanostatic charge/discharge curves at 5 mA cm^{-2} for $NiCo_2O_4$/NF and NiNW@$NiCo_2O_4$/NF electrodes. **(C)** CV curves at different rate scans and **(D)** galvanostatic charge/discharge curves at different current densities for NiNW@$NiCo_2O_4$/NF electrodes.

curves of the $NiCo_2O_4$/NF and Ni NW@$NiCo_2O_4$/NF at the current density of 5 mA cm^{-2} are shown in **Figure 5B**. The comparisons of **Figures 5A,B** indicate a higher capacitance of NiNW@$NiCo_2O_4$/NF, which can be attributed to the less aggregation of active materials and more active sites provided by the novel 3D hierarchical core–shell nanostructure due to the introduction of nickel nanowires. The areal specific capacitance (F cm^{-2}) of electrodes can be calculated according to the following equation (Wei et al., 2016):

$$C = Jt / \Delta V \tag{3}$$

where J is the current density (A cm^{-2}), t represents the discharge time (s), and ΔV designate the voltage window (V) for the galvanostatic charge–discharge measurements. By the calculation, the areal specific capacitance of $NiCo_2O_4$/NF is 3.5 F cm^{-2} at the current density of 5 mA cm^{-2}, however, those of NiNW@$NiCo_2O_4$/NF is reach up to 7.4 F cm^{-2} at the same current density. **Figure 5C** shows the typical CV curves of NiNW@$NiCo_2O_4$/NF under different sweep rates. As shown in **Figure 5D**, almost symmetric curves are observed during the charge/discharge processes under deferent current densities, indicating a good electrochemical capacitive characteristic and excellent reversible redox property.

Figure 6A presents the relationship between areal specific capacitance and current density of NiNW@$NiCo_2O_4$/NF and $NiCo_2O_4$/NF electrodes. The areal specific capacitances of NiNW@NiCo-NR/NF electrode are 7.44, 7.07, 6.88, 6.80, 6.73, 6.70, 6.65, 6.64, 6.55, and 6.55 F cm^{-2} at different current densities of 5, 10, 15, 20, 25, 30, 40, 50, 75, and 100 mA cm^{-2}, respectively. This manifests that almost 88.04% of the areal specific capacitance is still retained after the current density increases from 5 to 100 mA cm^{-2}, which is evidently higher than that of NiCo-NR/NF electrode (47.46%), suggesting a better rate capability of NiNW@$NiCo_2O_4$/NF electrode which is attributed to the shorter ion

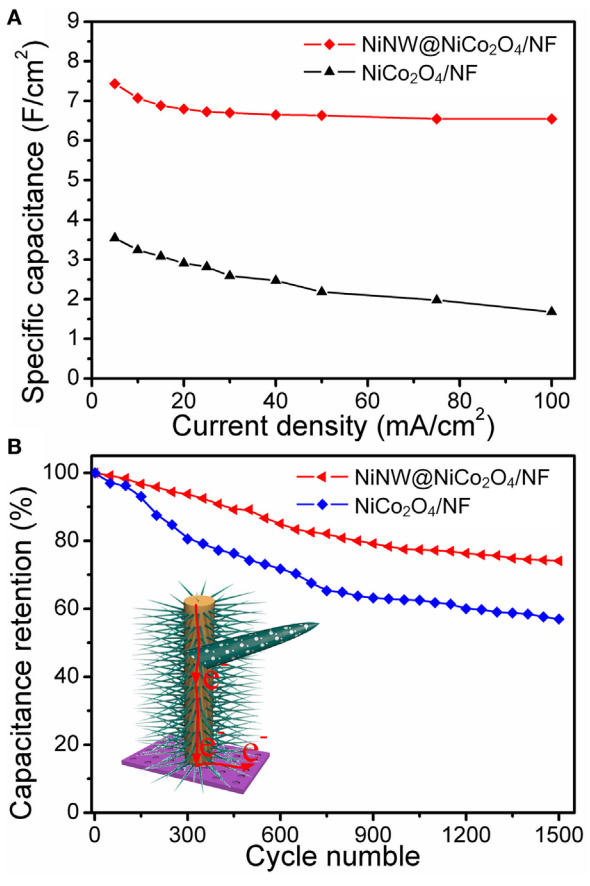

FIGURE 6 | **(A)** Specific capacitance values of $NiCo_2O_4$/NF and NiNW@$NiCo_2O_4$/NF as a function of current densities. **(B)** Cycling performance at progressively varying current densities.

channels provided by the growth of $NiCo_2O_4$ nanorods nanoarrays on the surface of prickly nickel nanowires than smooth nickel foam. The cycling stability of NiNW@$NiCo_2O_4$/NF and $NiCo_2O_4$/NF electrode were evaluated by the galvanostaic charge/discharge measurements for 1,500 cycles at a constant current density of 25 mA cm^{-2}, as shown in **Figure 6B**. It can be seen that both plots are gradually decreasing with the increase of cycle times. However, the downward trend of NiNW@$NiCo_2O_4$/NF electrode is more moderate than that of $NiCo_2O_4$/NF electrode, which can be owing to the buffer action in adsorption/desorption process due to the presence of nickel nanowires.

CONCLUSION

In summary, a novel 3D hierarchical core–shell structured NiNW@$NiCo_2O_4$/NF electrode was successfully fabricated by a facile method. The results indicate that the nickel nanowire@$NiCo_2O_4$/Ni foam electrode shows a high areal specific capacitance (7.4 F cm^{-2} at 5 mA cm^{-2}), excellent rate capability and good cycling stability. The superior electrochemical properties made it promising as electrode for supercapacitors. And this work provides a feasible way to improve rate performance.

AUTHOR CONTRIBUTIONS

HW and LL participated in the experiment and wrote the article. XL participated in the experiment and drew the scheme and figures. HW conceived and supervised the project and revised the manuscript. All authors contributed to the general discussion.

ACKNOWLEDGMENTS

This work is partially supported by the National Natural Science Foundation of China (NSFC, No. 11574077) and the Natural Science Foundation of Hubei Province of China (No. 2016CFB102).

SUPPLEMENTARY MATERIAL

The Supplementary Material for this article can be found online at http://www.frontiersin.org/article/10.3389/fenrg.2017.00033/full#supplementary-material.

REFERENCES

Chen, J. S., Guan, C., Gui, Y., and Blackwood, D. J. (2017). Rational design of self-supported Ni_3S_2 nanosheets array for advanced asymmetric supercapacitor with a superior energy density. *ACS Appl. Mater. Interfaces* 9, 496–504. doi:10.1021/acsami.6b14746

Cheng, J., Yan, H., Lu, Y., Qiu, K., Hou, X., Xu, J., et al. (2015). Mesoporous $CuCo_2O_4$ nanograsses as multi-functional electrodes for supercapacitors and electro-catalysts. *J. Mater. Chem. A* 3, 9769–9776. doi:10.1039/c5ta00408j

Chou, S.-L., Wang, J.-Z., Chew, S.-Y., Liu, H.-K., and Dou, S.-X. (2008). Electrodeposition of MnO_2 nanowires on carbon nanotube paper as free-standing, flexible electrode for supercapacitors. *Electrochem. commun.* 10, 1724–1727. doi:10.1016/j.elecom.2008.08.051

Deng, T., Zhang, W., Arcelus, O., Kim, J. G., Carrasco, J., Yoo, S. J., et al. (2017). Atomic-level energy storage mechanism of cobalt hydroxide electrode for pseudocapacitors. *Nat. Commun.* 8, 15194. doi:10.1038/ncomms15194

Hu, B., Qin, X., Asiri, A. M., Alamry, K. A., Al-Youbi, A. O., and Sun, X. (2013). Fabrication of $Ni(OH)_2$ nanoflakes array on Ni foam as a binder-free electrode material for high performance supercapacitors. *Electrochim. Acta* 107, 339–342. doi:10.1016/j.electacta.2013.06.003

Kim, H. S., Cook, J. B., Lin, H., Ko, J. S., Tolbert, S. H., Ozolins, V., et al. (2017). Oxygen vacancies enhance pseudocapacitive charge storage properties of MoO_{3-x}. *Nat. Mater.* 16, 454–460. doi:10.1038/nmat4810

Lai, F., Huang, Y., Miao, Y.-E., and Liu, T. (2015). Controllable preparation of multi-dimensional hybrid materials of nickel-cobalt layered double hydroxide nanorods/nanosheets on electrospun carbon nanofibers for high-performance supercapacitors. *Electrochim. Acta* 174, 456–463. doi:10.1016/j.electacta.2015.06.031

Lei, Y., Li, J., Wang, Y., Gu, L., Chang, Y., Yuan, H., et al. (2014). Rapid microwave-assisted green synthesis of 3D hierarchical flower-shaped $NiCo_2O_4$ microsphere for high-performance supercapacitor. *ACS Appl. Mater. Interfaces* 6, 1773–1780. doi:10.1021/am404765y

Li, L., Liu, X., Liu, C., Wan, H., Zhang, J., Liang, P., et al. (2018). Ultra-long life nickel nanowires@nickel-cobalt hydroxide nanoarrays composite pseudocapacitive electrode: construction and activation mechanism. *Electrochim. Acta* 259, 303–312. doi:10.1016/j.electacta.2017.10.190

Li, X., Jiang, L., Zhou, C., Liu, J., and Zeng, H. (2015). Integrating large specific surface area and high conductivity in hydrogenated $NiCo_2O_4$ double-shell hollow spheres to improve supercapacitors. *NPG Asia Mater.* 7, e165. doi:10.1038/am.2015.11

Li, X., Xue, H., and Pang, H. (2017a). Facile synthesis and shape evolution of well-defined phosphotungstic acid potassium nanocrystals as a highly efficient visible-light-driven photocatalyst. *Nanoscale* 9, 216. doi:10.1039/c6nr07680g

Li, B., Gu, P., Feng, Y., Zhan, G., Huang, K., Xue, H., et al. (2017b). Ultrathin nickel-cobalt phosphate 2D nanosheets for electrochemical energy storage under aqueous/solid-stateelectrolyte. *Adv. Funct. Mater.* 27, 1605784. doi:10.1002/adfm.201605784

Li, W.-H., Ding, K., Tian, H.-R., Yao, M.-S., Nath, B., Deng, W.-H., et al. (2017c). Conductive metal-organic framework nanowire array electrodes for high-performance solid-state supercapacitors. *Adv. Funct. Mater.* 27, 1702067. doi:10.1002/adfm.201702067

Liu, X., Shi, S., Xiong, Q., Li, L., Zhang, Y., Tang, H., et al. (2013). Hierarchical $NiCo_2O_4$@ $NiCo_2O_4$ core/shell nanoflake arrays as high-performance supercapacitor materials. *ACS Appl. Mater. Interfaces* 5, 8790–8795. doi:10.1021/am402681m

Liu, Y., Fu, N., Zhang, G., Xu, M., Lu, W., Zhou, L., et al. (2017). Design of hierarchical NiCo@NiCo layered double hydroxide core-shell structured nanotube array for high-performance flexible all-solid-state battery-type supercapacitors. *Adv. Funct. Mater.* 27, 1605307. doi:10.1002/adfm.201605307

Lu, X., Zheng, D., Zhai, T., Liu, Z., Huang, Y., Xie, S., et al. (2011). Facile synthesis of large-area manganese oxide nanorod arrays as a high-performance electrochemical supercapacitor. *Energy Environ. Sci.* 4, 2915. doi:10.1039/c1ee01338f

Pu, J., Wang, T., Wang, H., Tong, Y., Lu, C., Kong, W., et al. (2014). Direct growth of $NiCo_2S_4$ nanotube arrays on nickel foam as high-performance binder-free electrodes for supercapacitors. *ChemPlusChem* 79, 577–583. doi:10.1002/cplu.201300431

Shang, Y., Gai, Y., Wang, L., Hao, L., Lv, H., Dong, F., et al. (2017). A facile and effective method for constructing rambutan-like $NiCo_2O_4$ hierarchical architectures for supercapacitor applications. *Eur. J. Inorg. Chem.* 17, 2340–2346. doi:10.1002/ejic.201700020

Shen, L., Yu, L., Yu, X. Y., Zhang, X., and Lou, X. W. (2015). Self-templated formation of uniform $NiCo_2O_4$ hollow spheres with complex interior structures for lithium-ion batteries and supercapacitors. *Angew. Chem. Int. Ed. Engl.* 54, 1868–1872. doi:10.1002/anie.201409776

Shi, M., Yang, C., Song, X., Zhao, L., Liu, J., Zhang, P., et al. (2017). Integrated sustainable wind power harvesting and ultrahigh energy density wire-shaped supercapacitors based on vertically oriented nanosheet-array-coated carbon fibers. *Adv. Sust. Syst.* 1, 1700044. doi:10.1002/adsu.201700044

Sun, H., Mei, L., Liang, J., Zhao, Z., Lee, C., Fei, H., et al. (2017). Three-dimensional holey-graphene/niobia composite architectures for ultrahigh-rate energy storage. *Science* 356, 599–604. doi:10.1126/science.aam5852

Tang, C. H., Yin, X., and Gong, H. (2013). Superior performance asymmetric supercapacitors based on a directly grown commercial mass 3D Co_3O_4@ $Ni(OH)_2$ core-shell electrode. *ACS Appl. Mater. Interfaces* 5, 10574–10582. doi:10.1021/am402436q

Wei, J. S., Ding, H., Zhang, P., Song, Y. F., Chen, J., Wang, Y. G., et al. (2016). Carbon dots/$NiCo_2O_4$ nanocomposites with various morphologies for high performance supercapacitors. *Small* 12, 5927–5934. doi:10.1002/smll.201602164

Wei, Q., Xiong, F., Tan, S., Huang, L., Lan, E. H., Dunn, B., et al. (2017). Porous one-dimensional nanomaterials: design, fabrication and applications in electrochemical energy storage. *Adv. Mater.* 29:1602300. doi:10.1002/adma.201602300

Xia, W., Qu, C., Liang, Z., Zhao, B., Dai, S., Qiu, B., et al. (2017). High-performance energy storage and conversion materials derived from a single metal-organic framework/graphene aerogel composite. *Nano Lett.* 17, 2788–2795. doi:10.1021/acs.nanolett.6b05004

Xiao, X., Ding, T., Yuan, L., Shen, Y., Zhong, Q., Zhang, X., et al. (2012). WO_{3-x}/MoO_{3-x}core/shell nanowires on carbon fabric as an anode for all-solid-state asymmetric supercapacitors. *Adv. Energy Mater.* 2, 1328–1332. doi:10.1002/aenm.201200380

Yuan, C., Li, J., Hou, L., Zhang, X., Shen, L., and Lou, X. W. D. (2012). Ultrathin mesoporous $NiCo_2O_4$ nanosheets supported on Ni foam as advanced electrodes for supercapacitors. *Adv. Funct. Mater.* 22, 4592–4597. doi:10.1002/adfm.201200994

Zhang, G. Q., Wu, H. B., Hoster, H. E., Chan-Park, M. B., and Lou, X. W. (2012). Single-crystalline $NiCo_2O_4$ nanoneedle arrays grown on conductive substrates as binder-free electrodes for high-performance supercapacitors. *Energy Environ. Sci.* 5, 9453. doi:10.1039/c2ee22572g

Zheng, S., Xue, H., and Pang, H. (2017a). Supercapacitors based on metal coordination materials. *Coord. Chem. Rev.* doi:10.1016/j.ccr.2017.07.002

Zheng, S., Li, X., Yan, B., Hu, Q., Xu, Y., Xiao, X., et al. (2017b). Transition-metal (Fe, Co, Ni) based metal-organic frameworks for electrochemical energy storage. *Adv. Energy Mater.* 7, 1602733. doi:10.1002/aenm.201602733

Conflict of Interest Statement: The authors declare that the research was conducted in the absence of any commercial or financial relationships that could be construed as a potential conflict of interest.